ELSEVIER

Ceramics International 27 (2001) 269–276

CERAMICS INTERNATIONAL

www.elsevier.com/locate/ceramint

# The influence of alumina addition and its distribution upon grain-boundary conduction in 15 mol.% calcia-stabilized zirconia

Jong-Heun Lee *, Toshiyuki Mori, Ji-Guang Li, Takayasu Ikegami, Satoshi Takenouchi

*National Institute for Research in Inorganic Materials, Namiki 1-1, Tsukuba, Ibaraki 305-0044, Japan*

Received 18 April 2000; received in revised form 28 April 2000; accepted 23 May 2000

**Abstract**

The improvement of grain-boundary conduction was studied in 15 mol.% calcia-stabilized zirconia (15CSZ) by adding $Al_2O_3$ in the forms of fine powder and single crystalline particles sized 4–10 μm as a scavenger for resistive siliceous phase. The addition of 1 mol.% $Al_2O_3$ improved the grain-boundary conduction when sintered at $<1500°C$, whereas it deteriorated at $>1550°C$. The restraining $Al_2O_3$ dissolution into inter-granular glass phase was a key feature for maximizing the scavenging efficiency. At 1450°C, the addition of single crystalline $Al_2O_3$ sized 4 and 10 μm enhanced grain-boundary conductivity by a factor of 14–16, whose enhancement was about twice of that by fine $Al_2O_3$ powder. It can be explained by the combination of the sufficient reaction path assisted by fast grain-boundary diffusion and the restraining glass phase formation by employing coarse and inactive single crystalline $Al_2O_3$ particles. 

*Keywords:* B. Grain boundaries; C. Ionic conductivity; C. Impedance; Calcia-stabilized zirconia

## 1. Introduction

The grain-boundary conduction becomes important especially at low temperatures in the stabilized zirconia, the representative ionic conductor. The space charge layer [1] and the resistive siliceous film at the grain boundary [2,3] usually explain the origins of grain-boundary resistance in the intrinsic and extrinsic light, respectively.

The siliceous grain-boundary phase plays dominant role when the sample is impure. However, even a small concentration of silica is known to deteriorate the grain-boundary conduction to a large extent [4–7]. Therefore, it is hard to avoid the detrimental effect of siliceous impurities even at a relatively pure sample because $SiO_2$ is the most ubiquitous background impurity in the ceramic processing. The present authors [8] have reported that 120 ppm of $SiO_2$ in the starting 8 mol.% yttria-stabilized zirconia (8YSZ) powder results in segregation of $^{28}Si^-$ at grain boundary of sintered body using imaging secondary ion mass spectroscopy (SIMS).

As a convenient approach to improve grain-boundary conduction, various additives including $Fe_2O_3$ [9], $Bi_2O_3$ [9] and $Al_2O_3$ [6,9–18] were tried. The $Al_2O_3$ is acknowledged as the most effective one [12,14–16] to scavenge the siliceous grain-boundary phase although there are also a few controversial results [9,19]. However, the reports on the scavenging by $Al_2O_3$ are usually concentrated on 8YSZ.

Aoki et al. [4] studied correlation between solute segregation and grain-boundary conduction in 15 mol.% calcia-stabilized zirconia (15CSZ) containing $<80$ ppm Si using scanning transmission electron microscopy. They reported that the specific grain-boundary conductivity is $10^3$ less than grain-interior one even at one monolayer of silicon and calcium segregation at the grain boundary. The segregation of siliceous phase at grain boundary in calcia-stabilized zirconia (CSZ) could be found elsewhere [2,20,21]. Nevertheless, $Al_2O_3$ addition to CSZ was scarcely tried to improve the grain-boundary conduction.

In this study, the improvement of grain-boundary conduction was studied in 15CSZ by adding 1 mol.%

* Corresponding author at current address: School of Materials Science and Engineering, Seoul National University, Seoul 151-742, South Korea. Tel.: +82-2-880-6981; fax: +82-2-884-1413.

*E-mail address:* jonghuen@gong.snu.ac.kr (J.-H. Lee).

0272-8842/01/$20.00 
PII: S0272-8842(00)00075-4

$Al_2O_3$ in the forms of fine powder and single crystalline particles sized 4.4 and 10 μm. The change in the grain-boundary conduction, by varying the distribution, size, location and inter-particle spacing of $Al_2O_3$ particles, was studied in order to find the criteria for effective scavenging. Finally, the mechanism of scavenging by $Al_2O_3$ was suggested from the correlation between grain-boundary resistivity, sintering temperatures and the reaction of $Al_2O_3$ with inter-granular phase.

## 2. Experimental procedures

The 15 mol.% calcia-stabilized zirconia powders (CSZ-15 Heat-treated, Daiichi Kigenso Kagaku Kogyo Co. Ltd, Osaka, Japan) was used as a raw materials. The concentrations of impurities $SiO_2$, $TiO_2$, $Fe_2O_3$, and $Na_2O$ were quoted as 0.05, 0.11, 0.023, and 0.02 wt.%. The $Al_2O_3$ powder sized 0.3 μm (AKP30, Sumitomo Chemical Co., Tokyo, Japan) was employed for dispersion of fine particles. In order to get the distribution of coarse $Al_2O_3$ particles in 15CSZ, it is undesirable to apply the secondary particle consisting of many small primary ones because it might fragment during the mixing process. Therefore, the single crystalline $Al_2O_3$ particles sized 4.4 and 10 μm (AA4 and AA10, Sumitomo Chemical Co., Tokyo, Japan) with mono-dispersed distribution were used in this study.

A combination of 15CSZ, $Al_2O_3$, and $C_2H_5OH$ was vigorously stirred for 1 h with ultrasonic vibration for good dispersion. The ball milling procedures was avoided in order to prevent the crushing of the coarse $Al_2O_3$ particles. The solvent was removed by rotatory evaporator at 80°C and the aggregates were dried at 120°C for 24 h. The soft aggregation was pulverized with stainless steel sieve and Teflon spoon. A 15CSZ powder was also prepared with the 1 h of ultrasonic dispersion as a control, to eliminate the different background-impurity levels present both with and without ultrasonic dispersion. Table 1 summarizes the sample specifications, source materials, and preparation method of starting powders. The subscript after 'A' means the average particle size of $Al_2O_3$ particles in μm.

Table 1
The specification, source materials and preparation method of the starting powders

| Sample | Source materials | Preparation |
|---|---|---|
| 15CSZ | 15CSZ powder | Ultrasonic dispersion for 1 h |
| 15CSZ–$1A_{03}$ | 15CSZ + 1 mol.% $Al_2O_3$ (0.3 μm) | Ultrasonic dispersion for 1 h |
| 15CSZ–$1A_4$ | 15CSZ + 1 mol.% $Al_2O_3$ (4.4 μm) | Ultrasonic dispersion for 1 h |
| 15CSZ–$1A_{10}$ | 15CSZ + 1 mol.% $Al_2O_3$ (10 μm) | Ultrasonic dispersion for 1 h |

The impurity levels of 15CSZ powders after ultrasonic dispersion were determined by inductively coupled plasma (ICP) emission spectroscopy (Model No. SPS1700, Sieko Co., Chiba, Japan). Table 2 shows the results. It can be seen that the impurity concentrations coincide well with the quoted ones.

The powders were uniaxially pressed into pellet and then isostatically pressed at 200 MPa. The crucible for sintering was fabricated using the identical 15CSZ powder in the laboratory and the green pellets were also covered with 15CSZ powder to avoid contamination from the furnace. The pellets were sintered at 1450–1600°C for 4 h in air atmosphere. All the samples were thermally etched at 1400°C for 1 h in order to observe the microstructures. For convenience, hereinafter, the samples will be denoted with the sample name and the sintering temperature. For examples, 15CSZ–$1A_{03}$–1475 means 15CSZ–$1A_{03}$ sintered at 1475°C for 4 h. The heating and cooling rates were fixed to 200°C/h. The apparent densities were measured by Archimedes' method. Platinum electrodes were applied to the pellet by removing of surface layer, coating of Pt paste (TR 7905, Tanaka Co., Tokyo, Japan), drying, and subsequent heat treatment at 1000°C for 1 h.

The average grain size was calculated using linear intercept method measuring more than 500 grains from scanning electron micrographs [22]. The complex impedance was measured by SI 1260 impedance/gain-phase analyzer (Model No. SI 1260, Solartron, Inc., Farnborough, UK).

## 3. Results and discussion

Fig. 1 shows the microstructures of 15CSZ with and without $Al_2O_3$ addition sintered at 1450°C. There was no abnormal grain growth that can affect the analysis based on brick-layer model [23]. The dark regions B and E represent the coarse $Al_2O_3$ particles sized 4.4 and 10 μm, respectively. On the other hand, the same sizes of pores were also found [C, D in Fig. 1(c) and F in Fig. 1(d)]. It is regarded as the sites that were fully occupied by $Al_2O_3$ particles at low temperatures. The pores with partly occupied by small $Al_2O_3$ particle support the above explanation [D in Fig. 1(c) and F in Fig. 1(d)]. It suggests that $Al_2O_3$ particles react partly with siliceous

Table 2
ICP analysis of 15 mol.% calcia-stabilized zirconia powders after ultrasonic dispersion

| Impurites | Analysis |
|---|---|
| $SiO_2$ | 0.05 wt% |
| $TiO_2$ | 0.1 wt% |
| $Fe_2O_3$ | < 100 ppm |
| $Al_2O_3$ | < 50 ppm |

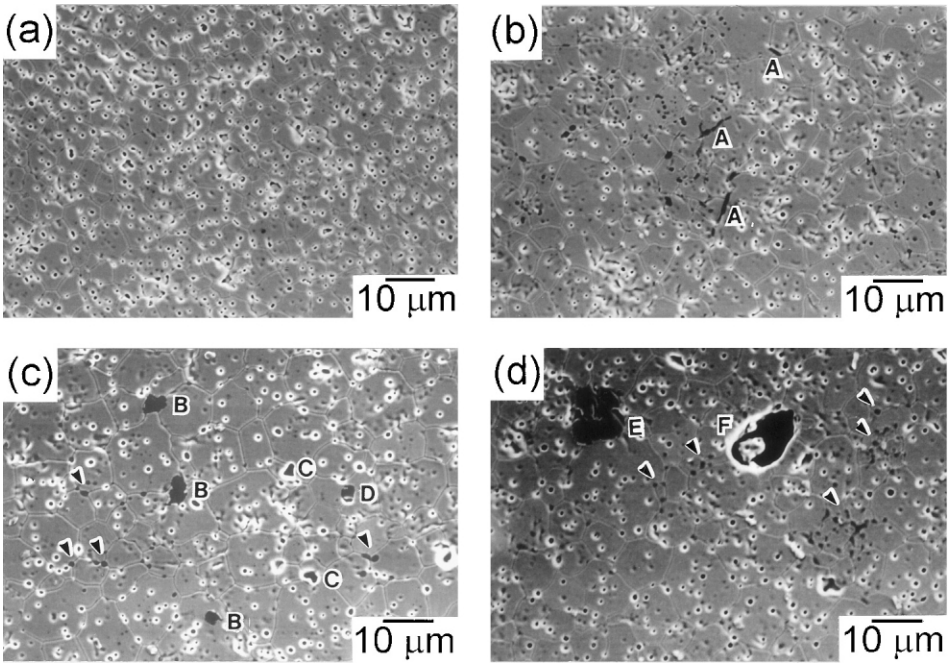


Fig. 1. The microstructures of 15CSZ with and without $Al_2O_3$ addition sintered at 1450°C for 4 h. (a) 15CSZ–1450, (b) 15CSZ–$1A_{03}$–1450, (c) 15CSZ–$1A_4$–1450, (d) 15CSZ–$1A_{10}$–1450.

grain-boundary phase at 1450°C. The schematic evaluation from low magnification SEM photos gives about 25 and 80 μm as the average spacing between coarse $Al_2O_3$ particles in 15CSZ–$1A_4$–1450 and 15CSZ–$1A_{10}$–1450, respectively.

The grain sizes and densities of samples are shown in Fig. 2. The density and grain size increased with adding $Al_2O_3$ regardless of their distributions. Radford and Bratton [20] studied the sintering behavior of 5 wt.% (10.4 mol.%) calcia-stabilized zirconia with various additives. They reported about 10% of density increments with adding 0.25 mol.% $SiO_2$, 5 mol.% $TiO_2$, and 1–2 mol.% $Al_2O_3$ when sintered at 1480°C. The density increased about 1–3% in the present study at 1475°C, which showed consistent tendency. The smaller density increment in this study might be related with the different amount of the co-existing minor impurities.

The complex impedance spectra were measured at 450°C in air and the results are shown in Figs. 3 and 4. Three semicircles at low, middle, and high frequencies represent the contributions of electrode polarization, grain boundary, and grain interior, respectively. From the rough calculation, specific grain-boundary resistivities ($\rho_{gb}^{sp}$) of all samples were estimated as about three to four orders of magnitude larger than grain-interior ones. Therefore, a series of three lumps of RC parallel circuit was assumed as an equivalent circuit because the parallel conduction contribution along the grain boundary can be neglected when one consider its thinness (about nm order) and high specific resistivity.

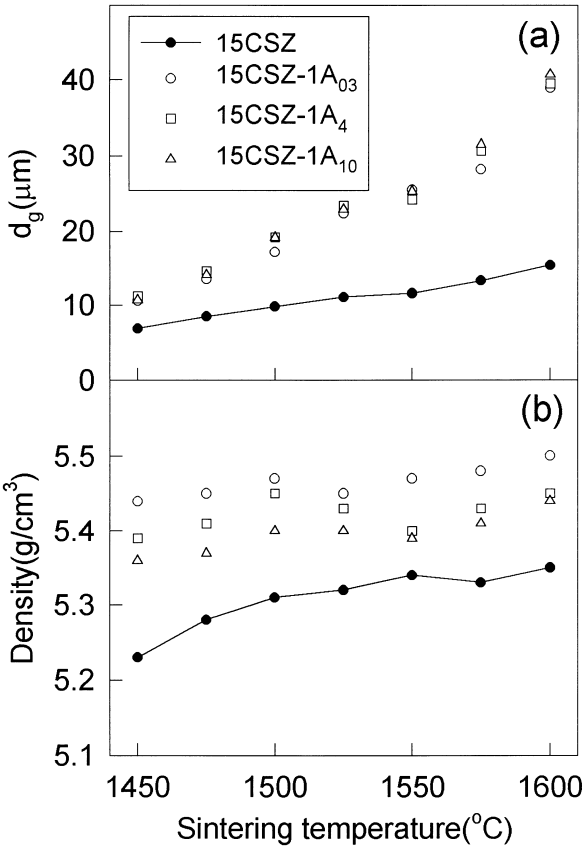


Fig. 2. The densities and average grain sizes ($d_g$) of samples with the variation of sintering temperatures. (a) Average grain size, (b) density.

Grain-interior and grain-boundary resistivities ($\rho_{gi}$ and $\rho_{gb}$) were deconvoluted from impedance spectra for analysis. For all the samples, $\rho_{gi}$ was constant as about 30 kΩ·cm, while $\rho_{gb}$ depended largely on the sintering temperature and $Al_2O_3$ distribution. In 15CSZ, $\rho_{gb}$ decreased systematically with increasing sintering temperatures. It resulted from the increase in grain size, that is, the decrease of the number of grain boundary per unit length. On the other hand, $\rho_{gb}$ of 15CSZ–$1A_{10}$–1450 is smaller than that of 15CSZ–1450 by a factor of about 1/25. The $\rho_{gb}$ decreased also remarkably at 1500 and 1550°C. However, when sintered at 1600°C, 15CSZ–$1A_4$ and 15CSZ–$1A_{10}$ did not show $\rho_{gb}$ decrement in comparison to 15CSZ, while 15CSZ–$1A_{03}$ still did. The reason will be discussed in the later section of this paper.

For the specific examination of scavenging efficiency, $\rho_{gb}$ was normalized because it depends upon the grain size ($d_g$), that is, the grain-boundary density. Resistance per unit grain-boundary area ($R_{gbs}$) was employed as a simple normalization method, which is given by the following equation [19]:

$$R_{gbs} = \rho_{gb}/D \quad (1)$$

where $D$ is the grain-boundary density (number/cm), the reciprocal of $d_g$.

Fig. 5 shows $\rho_{gb}$ and calculated $R_{gbs}$. The $R_{gbs}$ decreased largely from 35.4 Ω·cm² in 15CSZ–1450 to 2.2 Ω·cm² in 15CSZ–$1A_{10}$–1450. The $R_{gbs}$ decrement and increment in comparison to that of 15CSZ imply the improvement and deterioration of grain-boundary conduction, respectively. In order to comprehend the meaning of $R_{gbs}$ change, the following equations were considered. The specific grain-boundary resistivity ($\rho_{gb}^{sp}$) is given by the following equation [24]:

$$\rho_{gb}^{sp} = \rho_{gb}(d_g/\delta_{gb}) \quad (2)$$

where $\delta_{gb}$ is grain-boundary thickness. By combining (1) and (2), one can get the following Eq. (3) using the relationship, $d_g = 1/D$.

$$\rho_{gb}^{sp} = R_{gbs}/\delta_{gb}. \quad (3)$$

The $\rho_{gb}^{sp}$ value can be estimated if one assumed the typical thickness of siliceous film as 1 nm [4,25] and did not consider the effect of space charge layer. The calculated $\rho_{gb}^{sp}$ of 15CSZ–1450 and 15CSZ–$1A_{10}$–1450 were 354 and 22 MΩ·cm, which were about 11,800 and 730 times of $\rho_{gi}$ (about 30 kΩ·cm), respectively. It says that the 1 mol.% $Al_2O_3$ (sized 10 μm) addition decreases $\rho_{gb}^{sp}$ of 15CSZ–1450 by a factor of 1/16 by the scavenging reaction. The other $R_{gbs}$ change can be understood in the same light.

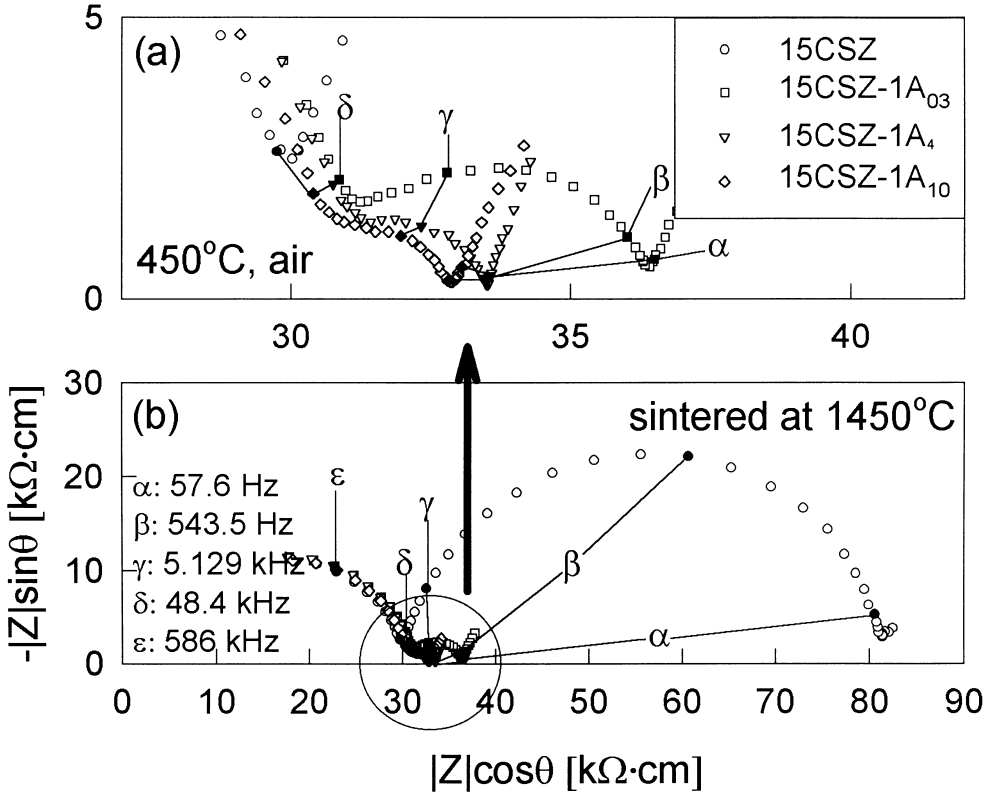


Fig. 3. The complex impedance spectra at 450°C of 15CSZ, 15CSZ–$1A_{03}$, 15CSZ–$1A_4$, and 15CSZ–$1A_{10}$ (sintering temperature: 1450°C), (a) enlarged one, (b) total view.

The scavenging factor (denoted as SF), dimensionless parameter for comparison, was defined as follows

$$SF = R_{gbs}/R_{gbs}(15CSZ) \quad (4)$$

where $R_{gbs}(15CSZ)$ is the $R_{gbs}$ of pure 15CSZ sample whose impurity level is identical to those with $Al_2O_3$ addition. The SF smaller than 1 means the improvement of grain-boundary conduction, which implies the scavenging of siliceous phase. The closer to 0 means the more effective scavenging. On the contrary, SF larger than 1 says the deterioration of grain-boundary conduction, which can result from the increase of resistive phase at grain boundary that blocks ionic conduction.

Fig. 6 shows the calculated SF. All the SF increases with sintering temperature and reaches to 1 at about 1525–1550°C. It says that the sintering temperatures lower than 1550°C are desirable for improving grain-boundary conduction. The SF becomes about 2 and 3 at 15CSZ–$1A_4$ and 15CSZ–$1A_{10}$ sintered at 1575 and 1600. The result indicates that $Al_2O_3$ addition increases the ion-blocking layer on the contrary at the high sintering temperatures.

Radford and Bratton [10] have reported the beneficial effect of $Al_2O_3$ upon the grain-boundary conduction of CSZ containing significant quantities of Si. They commented that $\rho_{gb}$ decreased slightly. In comparison, grain-boundary conduction at 1450–1500°C in the present study was improved markedly by adding $Al_2O_3$. The scavenging mechanism was discussed in relation with the reaction between $Al_2O_3$ and siliceous phase.

The present authors [26] have reported the influences of the identical three kinds of $Al_2O_3$ powders upon the scavenging in 8 mol.% yttria-stabilized zirconia although the $SiO_2$ impurity concentration is less (about 100–120 ppm) than that in this study. In summary, the followings were observed in SEM photos: (1) fine $Al_2O_3$ particles sized 0.5–1 μm were located both in the grain interior and the grain boundary always with a pointy shape; (2) coarse single crystalline $Al_2O_3$ particles sized 4.4 and 10 μm were located only at grain boundary. At least in the SEM observation, there was no distinct

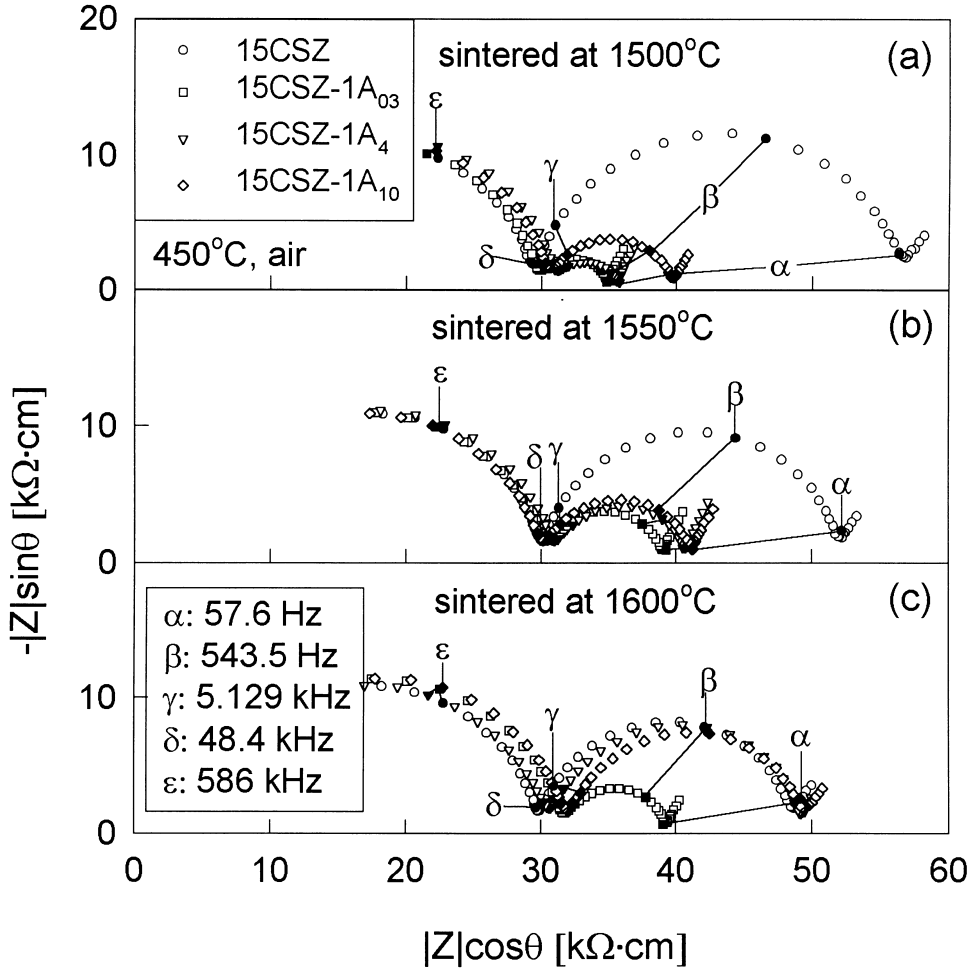


Fig. 4. The complex impedance spectra at 450°C of 15CSZ, 15CSZ–$1A_{03}$, 15CSZ–$1A_4$, and 15CSZ–$1A_{10}$ sintered at (a) 1500°C, (b) 1550°C and (c) 1600°C.

indication for dissolution of coarse $Al_2O_3$ into siliceous glass phase at 1500–1600°C.

In this study, the dark regions in Fig. 1(b), (c), and (d) are $Al_2O_3$ or that reacted with siliceous phase. Its location shows almost similar tendency with the previous study on 8YSZ. However, the followings features were different: (1) the fine $Al_2O_3$ particles were located more frequently on grain boundaries rather than in grain interior in 15CSZ–$1A_{03}$–1450; (2) the elongated dark region was found along the grain boundary in 15CSZ–$1A_{03}$–1450 [see A in Fig. 1(b)]; (3) the small dark grains besides 4 and 10 μm $Al_2O_3$ particles were found with a pointy shape in 15CSZ–$1A_4$–1450 and 15CSZ–$1A_{10}$–1450 [see arrows in Fig. 1(c) and (d)]. The results indicate that $Al_2O_3$ dissolves partly into inter-granular glass phase at 1450°C. It means that the dissolution of $Al_2O_3$ into inter-granular glass phase in CSZ–$Al_2O_3$ occurs at the lower temperatures than that in YSZ–$Al_2O_3$.

Shackelford et al. [21] studied the influence of silica addition upon the sintering of 3.5 wt% calcia-stabilized zirconia. They found the liquid phase rich in $SiO_2$ and CaO at grain boundary and suggested liquid phase sintering mechanism. Beekmans and Heyne [2] reported the two kinds of grain-boundary phase in 15 mol.% calcia-stabilized zirconia and analyzed the composition using microprobe analysis. One was rich in Ca, Si, and Al, while another was rich in Mg and Al. Both inter-granular phases were deficient in Zr.

Above results says that $Al_2O_3$ dissolves into inter-granular phase containing CaO and $SiO_2$. The minor impurities except $SiO_2$ can also involve in forming inter-granular phase. So it is not easy to identify the exact composition of inter-granular phase. However, for simplicity, the glass formation between CaO, $SiO_2$ and $Al_2O_3$ was considered as the probable framework. Many kinds of glassy phases are possible in CaO–$SiO_2$–$Al_2O_3$ system [27]. The lowest temperature that can form liquid phase is 1170°C although the composition is quite different from that in this study. Principally, if all the three components were homogeneously distributed over the samples, the liquid phase would not form at 1600°C because of very small concentrations of $SiO_2$ and $Al_2O_3$ in this study. However, many researchers have reported thin siliceous grain-boundary phase in stabilized zirconia system [2,6,11,16,21]. It is closely related with the segregation of siliceous phase at grain boundary and heterogeneous distribution of its concentrations over the samples.

In order to understand the reason why the SF decreased with increasing temperatures, the SEM microstructures of 15CSZ–$1A_{10}$ was examined with varying sintering temperatures, and the results were shown in Fig. 7. The $Al_2O_3$ particles sized 10 μm preserved their shape in 15CSZ–$1A_{10}$–1450 [see A in Fig. 7(a)]. It gradually dissolved into grain boundary with increasing temperatures to 1500 and then 1550°C [see irregular shaped particle C in Fig. 7(b) and the region D filled with dark inter-granular phase in Fig. 7(c)].

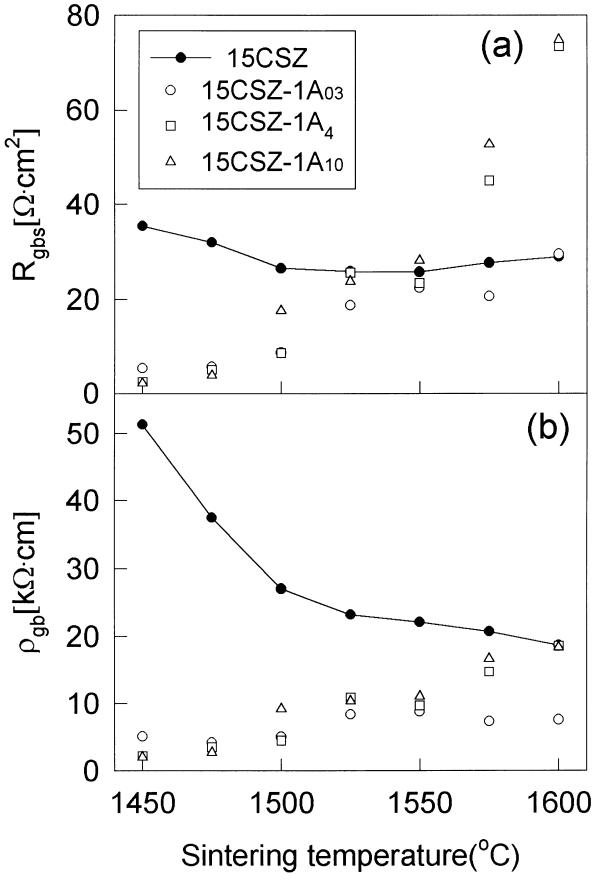


Fig. 5. The resistance per unit grain-boundary area ($R_{gbs}$) and grain-boundary resistivity ($\rho_{gb}$) with the variation of sintering temperatures. (a) $R_{gbs}$, (b) $\rho_{gb}$.

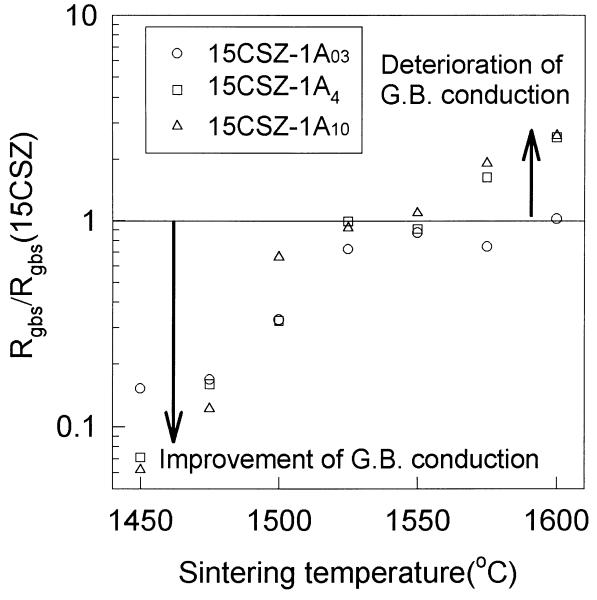


Fig. 6. The ratio of $R_{gbs}$ with $Al_2O_3$ addition over that without, as a criteria of scavenging efficiency, with varying sintering temperatures.

Finally, it can be seen that almost of the $Al_2O_3$ particles dissolved into grain boundary at 1600°C [Fig. 7(d)]. The $Al_2O_3$ dissolution reflects that the more glass phase is formed at the higher temperatures, which can explain the tendency of the decrease of scavenging efficiency (increase of SF in Fig. 6).

There are some differences in SF between the samples sintered at 1550–1600°C. That is, in this temperature regime, $R_{gbs}$ of 15CSZ–$1A_4$ and 15CSZ–$1A_{10}$ are about two to three times larger than that of 15CSZ, while $R_{gbs}$ of 15CSZ–$1A_{03}$ is almost same to that of 15CSZ. The reason is unclear at this point and should be studied more. However, one possible explanation is as follows: the larger amount of $Al_2O_3$ dissolution was observed in 15CSZ–$1A_{03}$ rather than in 15CSZ–$1A_4$ and 15CSZ–$1A_{10}$ at the fixed sintering temperatures although the microstructures were not presented. The different activities of $Al_2O_3$ might influence the dissolution behavior and the distribution of inter-granular phase that determine the ion blocking at the grain boundary.

It should be pointed out that $R_{gbs}$ of 15CSZ–$1A_{10}$–1450 and 15CSZ–$1A_4$–1450 are about half of that of 15CSZ–$1A_{03}$–1450. It is surprising if one considered that the finer $Al_2O_3$ particles with more frequency would have the more opportunity for scavenging reaction. Butler and Drennan [16] added 0.98 and 2.68 mol.% of $Al_2O_3$ to the $Y_2O_3/Yb_2O_3$ stabilized zirconia ceramics and examined its microstructures using TEM. They found that most intra-granular $Al_2O_3$ particle contained inclusion rich in Zr or Si plus Zr and that inter-granular one associated frequently with amorphous cusp rich in Si and Al. From the observation, they suggested that $Al_2O_3$ scavenged the siliceous second phase during the pinning time assisted by fast grain-boundary diffusion. The previous report [26] on 8YSZ showed that the scavenging efficiency was also not much different from each other between 8YSZ–$1A_{03}$ and 8YSZ–$1A_{10}$ although the former was slightly more efficient than the latter. The reason why the coarse $Al_2O_3$ with long inter-particle spacing showed the effective scavenging, was understood as the sufficient reaction path for scavenging assisted by fast grain-boundary diffusion. And it was proved by the $^{28}Si^-$ and $^{27}Al^{16}O^-$ concentration maps attained using imaging SIMS. Therefore, it can be thought that the sufficient reaction path by rapid grain-boundary diffusion plays an important role for the effective scavenging by coarse $Al_2O_3$ particles in this study.

Another important factor is the amount of liquid phase at 1450°C. From the phase diagram in CaO–$SiO_2$–$Al_2O_3$ system, it can be known that the decrease of $Al_2O_3$ content shows the tendency of diminishing the liquid phase. The coarse and inactive $Al_2O_3$ particles will result in the smaller dissolution into inter-granular phase rather than fine $Al_2O_3$ powder. In fact, as mentioned earlier, the elongated dark regions that reflect fluid inter-granular glass phase were frequently found in 15CSZ–$1A_{03}$–1450. On the other hand, almost of the small and dark regions in 15CSZ–$1A_4$–1450 and 15CSZ–$1A_{10}$–1450 showed the pointy morphology that reflects immobile grain-boundary phase. Therefore, the decrease of ion-blocking inter-granular phase due to the restraining $Al_2O_3$ dissolution explains the reason why the inactive single crystalline $Al_2O_3$ particles is more effective for scavenging.

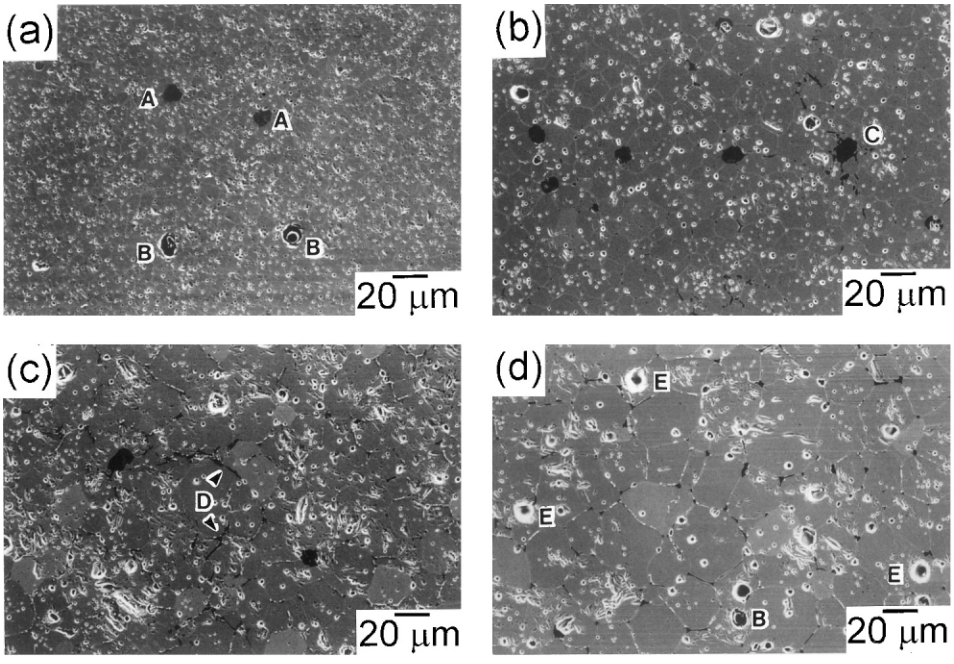


Fig. 7. The scanning electron micrographs of 15CSZ–$1A_{10}$ sintered at (a) 1450°C, (b) 1500 °C, (c) 1550 °C, and (d) 1600 °C for 4 h.

From the above discussion, the remarkable scavenging effect in 15CSZ–$1A_4$–1450 and 15CSZ–$1A_{10}$–1450, would be with the result of the desirable combination between the sufficient reaction path for scavenging reaction assisted by rapid grain-boundary diffusion and the restraining $Al_2O_3$ dissolution using inactive single crystalline $Al_2O_3$.

## 4. Conclusions

The influence of the size, distribution, and inter-particle distances of $Al_2O_3$ upon the grain-boundary conduction of 15 mol.% calcia-stabilized zirconia (15CSZ) was studied. Two different roles of $Al_2O_3$ were found. One is the improvement of grain-boundary conduction at $<1500°C$ by scavenging siliceous phase. The other is the deterioration at $>1550°C$ by forming more ion-blocking inter-granular phase. The most efficient scavenging was achieved by adding the single crystalline particles sized 4 and 10 μm at 1450°C. It enhanced the grain-boundary conductivity remarkably by a factor of 14-16 in spite of their long inter-particle spacing. The results can be interpreted as the combination of the sufficient reaction path for scavenging assisted by rapid grain-boundary diffusion and the restraining glass phase formation that involves $Al_2O_3$ dissolution using inactive and coarse single crystalline particles.

## Acknowledgements

One of the authors, Jong-Heun Lee, thanks to JIS-TEC/JST of Japan for an STA fellowship. The authors also thank to Daiichi Kigenso Kagaku Kogyo Co. Ltd. of Japan for providing CSZ-15 powder.

## References

[1] X. Guo, Physical origin of the intrinsic grain-boundary resistivity of stabilized-zirconia: role of the space-charge layers, Solid State Ionics 81 (1995) 235–242.
[2] N.M. Beekmans, L. Heyne, Correlation between impedance, microstructure and composition of calcia-stabilized zirconia, Electrochim. Acta 21 (1976) 303–310.
[3] S.P.S. Badwal, F.T. Ciacchi, S. Rajendran, J. Drennan, An investigation of conductivity, microstructure and stability of eletrolyte compositions in the system 9 mol% ($Sc_2O_3$–$Y_2O_3$)–$ZrO_2$($Al_2O_3$), Solid State Ionics 109 (1998) 167–186.
[4] M. Aoki, Y.-M. Chiang, I. Kosacki, J.-R. Lee, H. Tuller, Y. Liu, Solute segregation and grain-boundary impedance in high purity stabilized zirconia, J. Am. Ceram. Soc. 79 (1996) 1169–1180.
[5] S.P.S. Badwal, S. Rajendran, Effect of micro- and nano-structures on the properties of ionic conductors, Solid State Ionics 70/71 (1994) 83–95.
[6] M. Godickemier, B. Michel, A. Orliukas, P. Bohac, K. Sasaki, L. Gauckler, H. Henrich, P. Schwander, G. Kostorz, H. Hofmann, O. Frei, Effect of intergranular glass films on the electrical conductivity of 3Y-TZP, J. Mater. Res. 9 (1994) 1228–1240.
[7] M.L. Mecartney, Influence of an amorphous second phase on the properties of yttria-stabilized tetragonal zirconia ploycrystals (Y-TZP), J. Am. Ceram. Soc. 70 (1987) 54–58.
[8] J.-H. Lee, T. Mori, J.-G. Li, T. Ikegami, M. Komatsu, H. Haneda, Imaging secondary-ion mass spectroscopic observation of the scavenging siliceous film from 8-mol.%-yttria-stabilized zirconia by the addition of alumina, J. Am. Ceram. Soc. 83 (2000) 1273–1275.
[9] M.J. Verkerk, A.J.A. Winnubst, A.J. Burggraaf, Effect of impurities on sintering and conductivity of yttria-stabilized zirconia, J. Mater. Sci. 17 (1982) 3113–3122.
[10] K.C. Radford, R.J. Bratton, Zirconia electrolyte cells, Part 2 Electrical Properties, J. Mater. Sci. 14 (1979) 66–69.
[11] S. Rajendran, J. Drennan, S.P.S. Badwal, Effect of alumina additions on the grain boundary and volume resistivity of tetragonal zirconia polycrystals, J. Mater. Sci. Lett. 6 (1987) 1431–1434.
[12] A.J. Feighery, J.T.S. Irvine, Effect of alumina additions upon electrical properties of 8 mol.% yttria-stabilized zirconia, Solid State Ionics 121 (1999) 209–216.
[13] A. Yuzaki, A. Kishimoto, Effect of alumina dispersion on ionic conduction of toughened zirconia base composite, Solid State Ionics 116 (1999) 47–51.
[14] Y. Ji, J. Liu, Z. Lu, X. Zhao, T. He, W. Su, Study on the properties of $Al_2O_3$-doped $(ZrO_2)_{0.92}(Y_2O_3)_{0.08}$ electrolyte, Solid State Ionics 126 (1999) 277–283.
[15] X. Guo, C.-Q. Tang, R.-Z. Yuan, Grain boundary ionic conduction in zirconia-based solid electrolyte with alumina addition, J. Eur. Ceram. Soc. 15 (1995) 25–32.
[16] E.P. Butler, J. Drennan, Microstructural analysis of sintered high-conductivity zirconia with $Al_2O_3$ additions, J. Am. Ceram. Soc. 65 (1982) 474–478.
[17] J. Drennan, S.P.S. Badwal, The influence of $Al_2O_3$ additions to yttria-containing tetragonal zirconia polycrystals (Y-TZP): a microstructural and electrical conductivity study, in: S. Somiya, N. Yanagida, H. Yanagida (Eds.), Science and Technology of Zirconia III, American Ceramic Society, Colombus, OH, 1988, pp. 807–817.
[18] J.-H. Lee, T. Mori, J.-G. Li, T. Ikegami, M. Komatsu, H. Haneda, Improvement of grain-boundary conductivity of 8 mol.% yttria-stabilized zirconia by precursor scavenging of siliceous phase, J. Electrochem. Soc. 147 (2000) 2822–2829.
[19] M. Miyayama, H. Yanagida, A. Asada, Effect of $Al_2O_3$ addition on resistivity and microstructure of yttria-stabilized zirconia, Am. Ceram. Soc. Bull. 65 (1986) 660–664.
[20] K.C. Radford, R.J. Bratton, Zirconia electrolyte cells, Part 1 sintering studies, J. Mater. Sci. 14 (1979) 59–65.
[21] J.F. Shackelford, P.S. Nicholson, W.W. Smeltzer, Influence of $SiO_2$ on sintering of partially stabilized zirconia, Am. Ceram. Soc. Bull. 53 (1974) 865–867.
[22] M.I. Mendelson, Average grain size in polycrystalline ceramics, J. Am. Ceram. Soc. 52 (1969) 443–446.
[23] J. Fleig, J. Maier, The impedance of ceramics with highly resistive grain boundaries: validity and limits of the brick layer model, J. Eur. Ceram. Soc. 19 (1999) 693–696.
[24] M.J. Verkerk, B.J. Middelhuis, A.J. Burggraaf, Effect of grain boundaries on the conductivity of high-purity ceramics, Solid State Ionics 6 (1982) 159–170.
[25] D.R. Clarke, On the equilibrium thickness of intergranular glass phases in ceramic materials, J. Am. Ceram. Soc. 70 (1987) 15–22.
[26] J.-H. Lee, T. Mori, J.-G. Li, T. Ikegami, M. Komatsu, H. Haneda. The influence of alumina distributions upon scavenging highly resistive grain-boundary phase of 8 mol.% yttria-stabilized zirconia, Electrochemistry, 68 (2000) 120–125.
[27] Y.-M. Chiang, D.P. Birnie III, W.D. Kingery, Physical Ceramics, Wiley, New York, 1997, pp. 332–345.